c-JUN-mediated transcriptional responses in lymphatic endothelial cells are required for lung fluid clearance at birth

Siling Fu[a,b,1] 🆔, Yanxiao Wang[a,1], Ennan Bin[a], Huanwei Huang[a], Fengchao Wang[a,c] 🆔, and Nan Tang[a,b,c,2] 🆔

Fluid clearance mediated by lymphatic vessels is known to be essential for lung inflation and gas-exchange function during the transition from prenatal to postnatal life, yet the molecular mechanisms that regulate lymphatic function remain unclear. Here, we profiled the molecular features of lymphatic endothelial cells (LECs) in embryonic and postnatal day (P) 0 lungs by single-cell RNA-sequencing analysis. We identified that the expression of c-JUN is transiently upregulated in P0 LECs. Conditional knockout of *Jun* in LECs impairs the opening of lung lymphatic vessels at birth, leading to fluid retention in the lungs and neonatal death. We further demonstrated that increased mechanical pressure induces the expression of c-JUN in LECs. c-JUN regulates the opening of lymphatic vessels by modulating the remodeling of the actin cytoskeleton in LECs. Our study established the essential regulatory function of c-JUN-mediated transcriptional responses in facilitating lung lymphatic fluid clearance at birth.

lymphatic endothelial cells | mechanical pressure | neonatal | lung fluid clearance | c-JUN

Mammals undergo striking changes during the transition from prenatal to postnatal life. In utero, the embryonic lungs breathe in the fluid required for airway branching morphogenesis and alveolar epithelial differentiation (1, 2); at birth, fluid in the airway lumen moves across the epithelium and accumulates in the lung interstitium. The interstitial fluid must then be cleared rapidly to ensure proper inflation of lungs with air to enable their gas-exchange function. Insufficient fluid clearance can cause transient tachypnea in newborns (3, 4). It has been established that the function of lung lymphatic vessels is essential for clearing lung fluid at birth, and mouse genetic studies have demonstrated that impaired embryonic lymphatic vessel development leads to fluid retention in the lungs and subsequently neonatal death (5).

Our knowledge of the lymphatic system has been greatly advanced in past decades (6–9). The lymphatic system contains a complex network of vessels that are lined by lymphatic endothelial cells (LECs). The unidirectional lymphatic vessels consist of blind-end lymphatic capillaries and collecting lymphatic vessels and function in maintaining fluid homeostasis (6–8). Excess interstitial fluid is initially taken up by lymphatic capillaries, converged in the collecting lymphatic vessels, and eventually transported into blood circulation (10). Abnormal fluid clearance functions of lymphatic vessels can lead to edema in various tissues (11–13). Seminal studies into the cellular mechanisms involved in lymphatic fluid uptake functions have demonstrated that lymphatic capillaries have specialized "button-like" junctions comprising buttons and flaps (14, 15). Interstitial fluid passes through the open space between flaps in button-like junctions and enters lymphatic vessels. Although these discoveries have revealed the cellular mechanisms controlling lymphatic fluid clearance, the molecular mechanisms that modulate lymphatic fluid clearance remain largely unknown.

Using single-cell RNA sequencing (scRNA-seq) analysis, mouse genetics, and transmission electron microscopy (TEM), we analyzed the features of the LECs in embryonic and postnatal day (P) 0 lungs and investigated the molecular mechanisms that control lung lymphatic function at birth. We found that P0 LECs show distinct molecular features and transiently express an activator protein 1 (AP-1) transcription factor, c-JUN. Conditional knockout of *Jun* in LECs results in lung fluid retention, failed lung inflation, and neonatal death. We further demonstrated that increased mechanical pressure induces the expression of c-JUN in LECs. c-JUN in LECs regulates the opening of flaps by modulating the remodeling of the actin cytoskeleton. Our study collectively demonstrates that c-JUN-mediated transcriptional responses in LECs are required for the fluid clearance function of lung lymphatic vessels during the transition from prenatal to postnatal life.

Results

AP-1 Transcription Factors Are Upregulated in P0 LECs.
The establishment of the lymphatic vessel network is a prerequisite for lymphatic functions at birth (5, 16). We first

Significance

In human newborns, insufficient lung fluid clearance leads to ineffective gas exchange, respiratory distress, and tachypnea. The normal function of pulmonary lymphatic vessels is essential for lung inflation and gas exchange at birth. However, the molecular mechanisms regulating the fluid clearance functions of pulmonary lymphatic vessels remain elusive. Our study demonstrated that c-JUN-mediated transcriptional responses in lymphatic endothelial cells (LECs) are indispensable for lung fluid clearance at birth. c-JUN, which is upregulated by increased mechanical pressure in P0 lungs, facilitates the opening of lymphatic vessels by modulating the remodeling of the actin cytoskeleton in LECs. Our study established the essential regulatory function of c-JUN-mediated transcriptional responses in facilitating lung lymphatic fluid clearance during the transition from prenatal to postnatal life.

[1]S.F. and Y.W. contributed equally to this work.

[2]To whom correspondence may be addressed. Email: tangnan@nibs.ac.cn.

characterized the development of the lymphatic vessel network in embryonic and P0 lungs. LECs can be specifically labeled by GFP using the *Prox1*-GFP mouse line (17). At embryonic day (E) 12.5, only a few LECs were observed around the main bronchi (*SI Appendix*, Fig. S1 *A* and *B*). At E14.5, scattered LECs were present within the lung parenchyma (Fig. 1*A* and *SI Appendix*, Fig. S1 *A* and *B*). At E16.5, LECs were connected and formed a tubular network (Fig. 1*A* and *SI Appendix*, Fig. S1 *A* and *B*). After E16.5, the lymphatic vessels had extended to the distal alveolar sac region with significantly increased area fraction and branch numbers (Fig. 1*A* and *SI Appendix*, Fig. S1 *A–C*). No

intraluminal valves—a specific structure of collecting lymphatic vessels (18–20)—were observed (*SI Appendix*, Fig. S1*A*).

To profile the molecular features of LECs, GFP⁺ CD31⁺ LECs from *Prox1*-GFP mouse lungs were isolated at E14.5, E16.5, E18.5, and P0 and then analyzed by scRNA-seq (*SI Appendix*, Fig. S1 *D* and *E*). After filtering, normalization, and removal of potential outliers, a total of 2,663 cells that expressed high levels of classic LEC markers, *Prox1* and *Flt4*, were used for subsequent analyses (Fig. 1*B* and *SI Appendix*, Fig. S1*F*).

A uniform manifold approximation and projection (UMAP)-based plot revealed the LECs presented as three distinct cell clusters
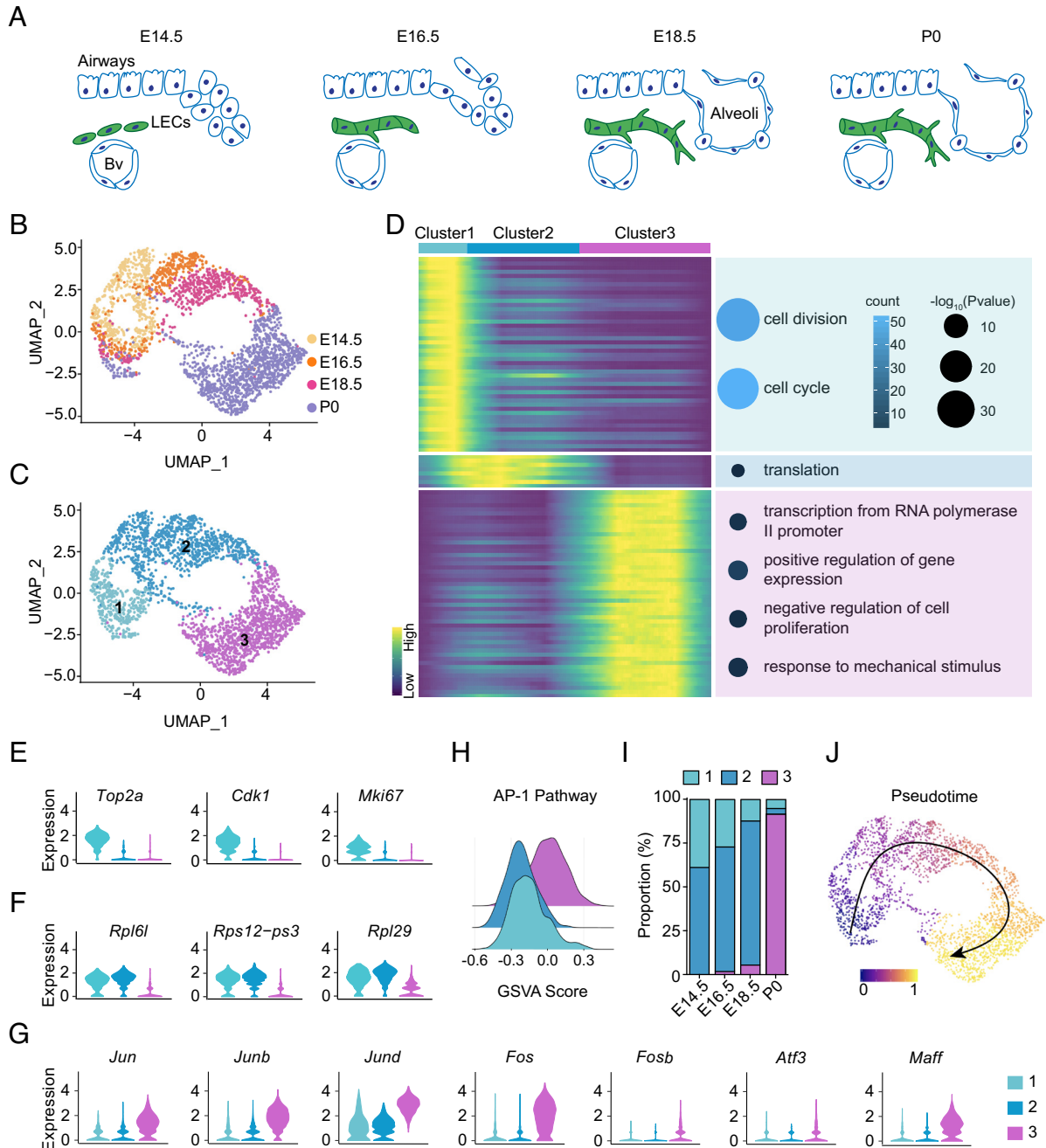

Fig. 1. AP-1 Transcription Factors Are Upregulated in P0 LECs. (*A*) Diagram to illustrate the development of lung lymphatic vessels. The lung lymphatic vessel network is established, in a proximal-to-distal manner, starting from E14.5. Bv: blood vessel. (*B*) UMAP plot of lung LECs obtained from different developmental stages. (*C*) The UMAP plot showing that lung LECs in (*B*) were clustered into three clusters. (*D*) Heatmap of differentially expressed genes in the three clusters of LECs (*Left*). Also shown are GO analyses of differentially expressed genes in the three clusters (*Right*). (*E*) Violin plots of selected genes highly expressed in Cluster 1 LECs. (*F*) Violin plots of selected genes highly expressed in Cluster 2 LECs. (*G*) Violin plots of AP-1 transcription factors highly expressed in Cluster 3 LECs. (*H*) Ridge plots for AP-1 pathway signatures based on GSVA scores in the LEC clusters. (*I*) The proportions of LECs from the three clusters among the various samples. (*J*) A pseudotime analysis with Slingshot and Monocle 2 represents the differentiation states of lung LECs proceeding from Cluster 1 to Cluster 3.

(Fig. 1 *B* and *C*). Differentially expressed genes in these clusters were used for gene ontology (GO) analysis to assess their differences (Dataset S1). The Cluster 1 LECs expressed high levels of genes with known functions in cell division and the cell cycle (e.g., *Top2a*, *Cdk1*, and *Mki67*) (Fig. 1 *D* and *E*). The high expression levels of S and G2/M phase markers indicated that the Cluster 1 LECs are actively proliferating LECs (*SI Appendix*, Fig. S1*G*). Cluster 2 LECs highly expressed a set of ribosome biogenesis genes that are also highly expressed in Cluster 1 LECs (Fig. 1 *D* and *F*). Cluster 3 LECs highly expressed genes involved in transcriptional regulation and mechanical responses (Fig. 1*D*). Compared with Cluster 1 and Cluster 2 LECs, the expression levels of a set of AP-1 transcription factors, including *Jun*, *Junb*, *Jund*, *Fos*, *Fosb*, *Atf3*, and *Maff*, were significantly increased in Cluster 3 LECs (Fig. 1*G*). Further, a gene set variation analysis (GSVA) indicated that genes involved in AP-1-mediated signaling pathways are enriched in Cluster 3 LECs (Fig. 1*H*).

The proportion of Cluster 1 LECs gradually decreased from E14.5 to P0 (Fig. 1*I*). Cluster 2 was the major LEC population in embryonic lungs: about 61% of LECs in embryonic lungs belong to Cluster 2 (Fig. 1*I*). Cluster 3 LECs accounted for over 90% of P0 LECs (Fig. 1*I*). In embryonic lungs, Cluster 3 LECs were not detected in the E14.5 LECs, and represented fewer than 6% of LECs in the E16.5 and E18.5 lungs (Fig. 1*I*). The pseudotime trajectory analyses of the three clusters using Slingshot and Monocle 2 indicated that there is a single development trajectory proceeding from Cluster 1 to Cluster 3 (Fig. 1*J*). Together, these results indicate that Cluster 1 and Cluster 2 LECs (the major clusters in embryonic lungs) are active in lymphangiogenesis, whereas Cluster 3 LECs (the major cluster in P0 lungs) may be responsible for the fluid clearance function of lymphatic vessels in P0 lungs.

c-JUN Is Transiently Upregulated in P0 LECs and Required for Lung Inflation at Birth. Our scRNA-seq results showed that the major LEC cluster in P0 lungs highly expresses AP-1 family genes, which behave as "immediate-early" genes and are rapidly transcribed in response to cellular stress (21). As a major component of the AP-1 family, c-JUN regulates a wide range of cellular processes (e.g., proliferation, differentiation, cell adhesion, and cell migration) in many organs and tissues (22–26). However, the function of c-JUN in LECs is unknown. We first conducted immunostaining to assess the protein expression of c-JUN in LECs. Consistent with our scRNA-seq results, only a few LECs expressed c-JUN in E16.5 and E18.5 lungs (Fig. 2 *A* and *B*). At P0, over 90% of LECs expressed c-JUN (Fig. 2 *A* and *B*). The proportion of c-JUN⁺ LECs dropped significantly at P1 and continued to drop to fewer than 5% in P62 adult lungs (Fig. 2 *A* and *B*). We also compared *JUN* expression in LECs collected from human neonate, child, and adult lungs (27). We found that the expression level of *JUN* in neonatal human lung LECs was the highest as compared to those in the child and adult lung LECs (*SI Appendix*, Fig. S2*A*). These results together demonstrate that the expression of c-JUN is transiently upregulated in LECs during the transition from prenatal to postnatal life.

We then deleted *Jun* in LECs to investigate whether c-JUN is required for the function of lung lymphatic vessels at birth. By treating pregnant female mice carrying *Prox1*-CreER;*Jun*^f/+^;*Rosa26*-mTmG (control) and *Prox1*-CreER;*Jun*^f/f^;*Rosa26*-mTmG (*Jun* cKO) embryos with tamoxifen at E16.5 and E17.5 (Fig. 2*C* and *SI Appendix*, Fig. S2*B*), *Jun* was efficiently deleted in P0 LECs (*SI Appendix*, Fig. S2 *C* and *D*).

Most (74%) of the control mice became pink in color and survived over 24 h (h), whereas over 73% (n = 27/37) of the *Jun* cKO mice appeared cyanotic and died within 24 h after birth (Fig. 2*D*). The network of lymphatic vessels in *Jun* cKO lungs was not

significantly affected, as assessed by quantification of lymphatic area fraction and branch numbers (*SI Appendix*, Fig. S3 *A* and *B*). Hematoxylin and eosin (H&E) staining indicated that the interstitium of *Jun* cKO lungs was thickened greatly, and the mean linear intercept (MLI) was significantly decreased compared with that in control lungs (Fig. 2 *E* and *F*). The Wet/Dry ratio of *Jun* cKO lungs was significantly higher than that of control lungs (Fig. 2*G*). These findings together support that deletion of *Jun* in LECs results in pulmonary edema and failed lung inflation at birth.

c-JUN in LECs Regulates Lung Fluid Clearance at Birth. We next investigated whether c-JUN regulates the fluid clearance function of lymphatic vessels. A previous study established that 40 kD dextran can be cleared by lymphatic vessels but not by blood vessels (28). We intratracheally injected P0 mice with 40 kD Cy7-conjugated dextran and then monitored the dextran signal using an in vivo imaging system (IVIS). The amount of Cy7-dextran in the region of the lungs was quantified as the values of radiant efficiency (*SI Appendix*, Fig. S3*C*). The values of radiant efficiency reduced significantly in P0 control lungs from post-injection 1 to 4 h, indicating that lymphatic vessels in neonatal mice are able to quickly clear fluid from lungs (Fig. 2 *H* and *I*). By contrast, in P0 *Jun* cKO lungs, the value of the radiant efficiency at post-injection 4 h was not significantly reduced as compared with that at post-injection 1 h (Fig. 2 *H* and *I*), supporting that lymphatic fluid clearance was impaired in *Jun* cKO lungs.

Button-like junctions are known to be essential for lymphatic fluid clearance (14). The button structure contains a set of tight junction molecules and cadherin molecules (14). The flaps indicate the overlapped edges of LECs between buttons (14). We further analyzed the structures of button-like junctions in control and *Jun* cKO lungs. Button-like junctions can be visualized by a discontinuous expression pattern of VE-Cadherin (VE-Cad) (14). We found that the formation of button-like junctions increased significantly from E18.5 to P0 in the LECs of control lungs (*SI Appendix*, Fig. S3 *D* and *E*). Note that the deletion of *Jun* in LECs did not affect the formation of button-like junctions at P0 (*SI Appendix*, Fig. S3 *D* and *E*). We then analyzed the opening of flaps by TEM. In P0 control lungs, 51% of flaps had an opening space larger than 0.05 μm² (Fig. 2 *J* and *K* and *SI Appendix*, Fig. S3*F*). In contrast, we found no flaps with an opening space larger than 0.05 μm² in *Jun* cKO lungs (Fig. 2 *J* and *K* and *SI Appendix*, Fig. S3*F*), demonstrating that *Jun* deletion impairs the opening of flaps in P0 LECs. Such impaired LEC flap opening may account for the failed lymphatic fluid clearance observed in the *Jun* cKO lungs.

To further evaluate the biological processes impacted by c-JUN in LECs, we performed RNA sequencing (RNA-seq) analysis of LECs isolated from P0 control and *Jun* cKO lungs and compared their differentially expressed genes (*SI Appendix*, Fig. S3*G* and Dataset S2). Interestingly, many downregulated genes in *Jun* cKO LECs are known to function in regulating cell adhesion, cytoskeleton organization, and cell shape change (*SI Appendix*, Fig. S3*H*). We also performed phalloidin staining on lung sections from P0 control and *Jun* cKO mice. The fluorescence intensity of phalloidin was significantly decreased in the P0 *Jun* cKO LECs compared to that in the P0 control LECs (*SI Appendix*, Fig. S3*I*), demonstrating the regulatory function of c-JUN in F-actin remodeling in lung LECs. To further evaluate the relationship between remodeling of the actin cytoskeleton in LECs and LEC flap opening, we injected P0 mice intratracheally with Cytochalasin D (CytoD), an inhibitor of actin polymerization. The TEM results showed that CytoD treatment significantly reduced the opening space of flaps, with only 8% of flaps having an opening space larger than 0.05 μm²
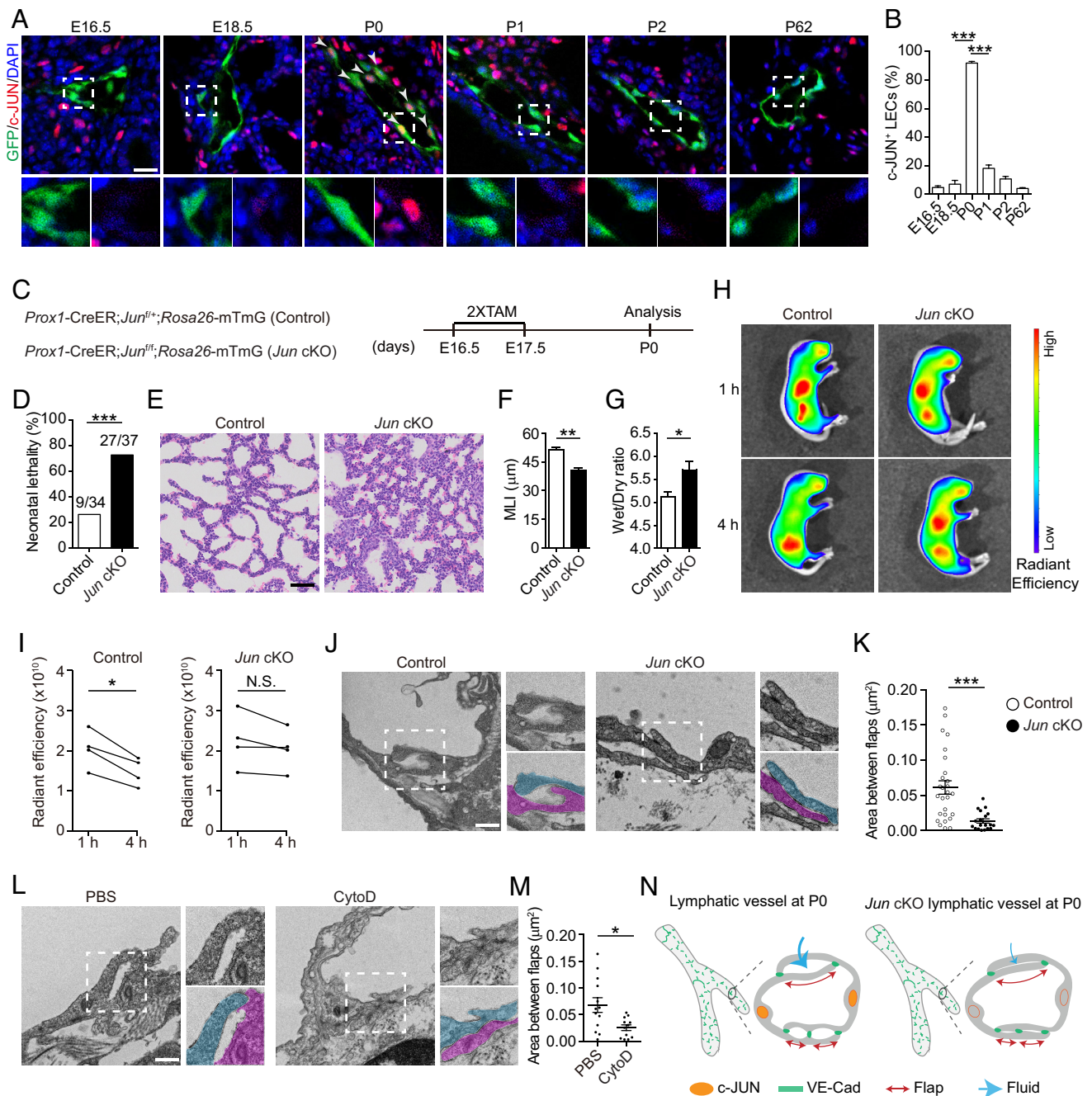
Fig. 2. c-JUN Is Transiently Upregulated in P0 LECs and Regulates Lung Fluid Clearance at Birth. (*A* and *B*) Lungs of *Prox1*-GFP mice were stained with antibodies against GFP and c-JUN (*A*). White arrowheads indicate c-JUN⁺ LECs. The percentages of c-JUN⁺ LECs were quantified (*B*) (mean ± SEM, n = 3). (*C*) *Prox1*-CreER; *Jun*^f/+^; *Rosa26*-mTmG (control) and *Prox1*-CreER; *Jun*^f/f^; *Rosa26*-mTmG (*Jun* cKO) mice were treated with tamoxifen (TAM) at E16.5 and E17.5. Analyses were performed at P0. (*D*) The percentages of neonatal lethality of control and *Jun* cKO mice. (*E* and *F*) Typical images of H&E-stained lung sections from P0 control and *Jun* cKO mice (*E*). MLIs were quantified (*F*) (mean ± SEM, n = 3). (*G*) Wet/Dry ratios of lungs from P0 control and *Jun* cKO mice (mean ± SEM, n = 6). (*H* and *I*) IVIS imaging of P0 control and P0 *Jun* cKO mice at 1 h and 4 h post 40 kD Cy7-dextran injection (*H*). The radiant efficiency value quantifications of 40 kD Cy7-dextran in the region of lungs at 1 h and 4 h (*I*) (mean ± SEM, n = 4). (*J* and *K*) TEM analysis of LECs in P0 control and *Jun* cKO lungs (*J*). The flaps of two LECs were magnified. Pseudocolors highlight two different LECs. Quantification of the area between flaps from TEM images (*K*) (mean ± SEM, n = 19 to 27 junctions). (*L* and *M*) TEM analysis of LECs in PBS- and CytoD-treated P0 control lungs (*L*). The flaps of two LECs were magnified. Pseudocolors highlight two different LECs. Quantification of the area between flaps from TEM images (*M*) (mean ± SEM, n = 12 to 13 junctions). (*N*) Diagram showing that deletion of *Jun* leads to impaired flap opening and defected fluid clearance of lymphatic vessels at birth. (N.S., not significantly different, *$P < 0.05$, **$P < 0.01$, ***$P < 0.001$, Student's *t* test. Scale bars: *A*, 15 μm; *E*, 50 μm; *J* and *L*, 500 nm.)

(Fig. 2 *L* and *M*), demonstrating that inhibiting remodeling of the actin cytoskeleton impaired LEC flap opening in P0 lungs. These results together suggest that c-JUN may control the remodeling of the actin cytoskeleton of LECs to facilitate the opening of LEC flaps, thereby promoting the fluid clearance function of lymphatic vessels (Fig. 2*N*).

Mechanical Pressure-Mediated c-JUN Expression Modulates Remodeling of the Actin Cytoskeleton in LECs. It has been proposed that the increased mechanical pressure that occurs in the tissue interstitium after fluid accumulation is one of the major forces driving interstitial fluid to the lymphatic vessels (29, 30). At birth, fluid from airways accumulates in the lung

interstitium, thus increasing the mechanical pressure in the lung interstitium (31). Our scRNA-seq results showed that genes that respond to mechanical stimulus are highly expressed in Cluster 3 LECs (Fig. 1*D*). We therefore investigated whether the expression of c-JUN in LECs is regulated by mechanical pressure. Following previously established protocols (32, 33), we cultured primary human lung LECs on substrata with different stiffness (*SI Appendix*, Fig. S4*A*). Immunostaining results showed that when LECs were cultured on the 0.3 kPa substratum (soft substratum), c-JUN expression was hardly detectable in LECs (Fig. 3 *A* and *B*). In LECs cultured on 0.9 kPa or above (hard substratum), over 90% of LECs showed strong c-JUN expression (Fig. 3 *A* and *B*). These results demonstrate that mechanical pressure can elevate c-JUN expression in LECs.

Given that many downregulated genes in *Jun* cKO LECs have functions related to regulating the cytoskeleton organization, we analyzed whether increased mechanical pressure can affect the remodeling of the actin cytoskeleton in LECs. The border of LECs was visualized by anti-VE-Cad staining. In LECs cultured on the soft substratum, the lateral sides of adjacent LECs adhered to each other, with smooth and linear VE-Cad lines and actin fibers running parallel to the lateral side of these LECs (Fig. 3 *C* and *D*). In LECs cultured on the hard substratum, the lateral sides of LECs were no longer held together, and the VE-Cad lines were interrupted, appearing jagged between the lateral sides of LECs (Fig. 3 *C* and *D*). Moreover, many actin fibers aligned parallel with these jagged VE-Cad lines in LECs cultured on the hard substratum

(Fig. 3 *C* and *D*). These results indicate that increased mechanical pressure can induce remodeling of the actin cytoskeleton in LECs.

We then investigated whether c-JUN modulates the remodeling of the actin cytoskeleton in LECs. Specifically, we treated LECs cultured on the hard substratum with scramble siRNA (siCtrl) or siRNA targeting *JUN* (si*JUN*). *JUN* siRNA treatment efficiently knocked down the expression of c-JUN in LECs (*SI Appendix*, Fig. S4 *B* and *C*). Unlike the jagged lateral sides of siCtrl LECs, the lateral sides of si*JUN* LECs were still held together (Fig. 3 *E*–*G*). Few jagged VE-Cad lines and actin fibers were observed between lateral sides of cells in si*JUN* LECs (Fig. 3 *E*–*G*). Additionally, the density of actin fibers was significantly reduced in si*JUN* LECs compared to the controls (Fig. 3 *E*–*G*). To further assess whether c-JUN-mediated remodeling of the actin cytoskeleton affects the permeability of LECs, we performed a transwell permeability assay on a confluent LEC monolayer. si*JUN* LECs showed significantly reduced permeability to 70 kD Tetramethylrhodamine-dextran as compared to siCtrl LECs (*SI Appendix*, Fig. S4*D*). Therefore, the transition from linear junctions to jagged junctions, which is mediated by c-JUN-regulated remodeling of the actin cytoskeleton, increases the permeability of LECs. We have previously demonstrated that the flap opening is controlled by c-JUN-mediated remodeling of the actin cytoskeleton. Although the jagged junctions in cultured LECs cannot fully recapitulate the LEC flap opening observed in P0 lungs, these results together support that c-JUN in LECs regulates the opening of flaps by modulating remodeling of the actin cytoskeleton.
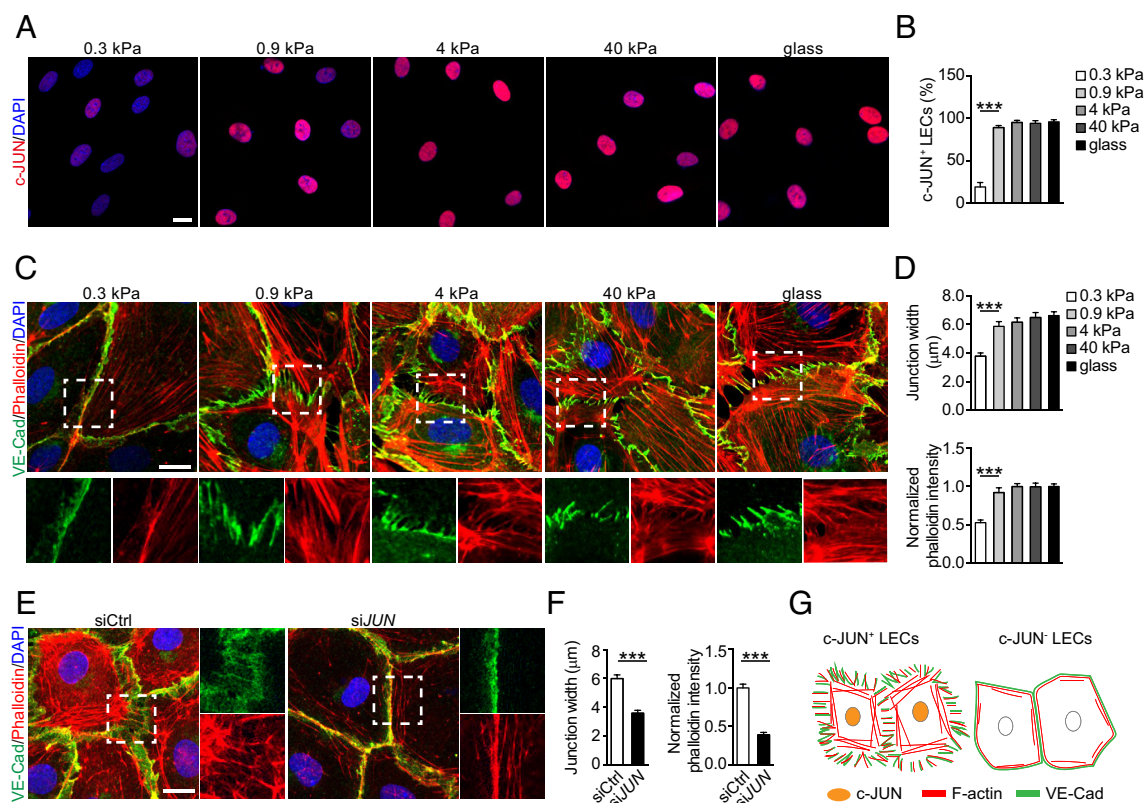

Fig. 3. Mechanical Pressure-Mediated c-JUN Expression Modulates Remodeling of the Actin Cytoskeleton in LECs. (*A* and *B*) LECs cultured on substrata with different stiffnesses were stained with an antibody against c-JUN (*A*). The percentages of c-JUN⁺ LECs were quantified (*B*) (mean ± SEM, n = 3). (*C* and *D*) LECs cultured on substrata with different stiffnesses were stained with phalloidin and an antibody against VE-Cad (*C*). The average junction width was quantified (*D*) (mean ± SEM, n ≥ 50 junctions). Relative average phalloidin intensity was quantified (*F*) (mean ± SEM, n ≥ 20 cells). (*E* and *F*) siCtrl or si*JUN* LECs were stained with phalloidin and an antibody against VE-Cad (*E*). The average junction width was quantified (*F*) (mean ± SEM, n ≥ 50 junctions). Relative average phalloidin intensity was quantified (*F*) (mean ± SEM, n ≥ 20 cells). (*G*) Diagram showing that c-JUN modulates remodeling of the actin cytoskeleton in LECs. (*P < 0.5, ***P < 0.001, Student's *t* test. Scale bars: *A*, *C*, and *E*, 15 μm.)

c-JUN Promotes CDH13 and ATF3 Expression. To identify the potential binding targets of c-JUN in LECs, we performed Cleavage Under Targets and Tagmentation (CUT&Tag) analysis using a c-JUN-specific antibody in LECs. After comparing peaks between siCtrl LECs and si*JUN* LECs, a total of 2,243 c-JUN binding peaks were identified (Fig. 4*A* and *SI Appendix*, Fig. S5*A*). A total of 1,501 candidate c-JUN binding genes were obtained after peak annotation (Dataset S3). The motif analysis showed that the most enriched motif is c-JUN binding motif (*SI Appendix*, Fig. S5*B*). We then filtered for candidate c-JUN binding genes that are both downregulated in
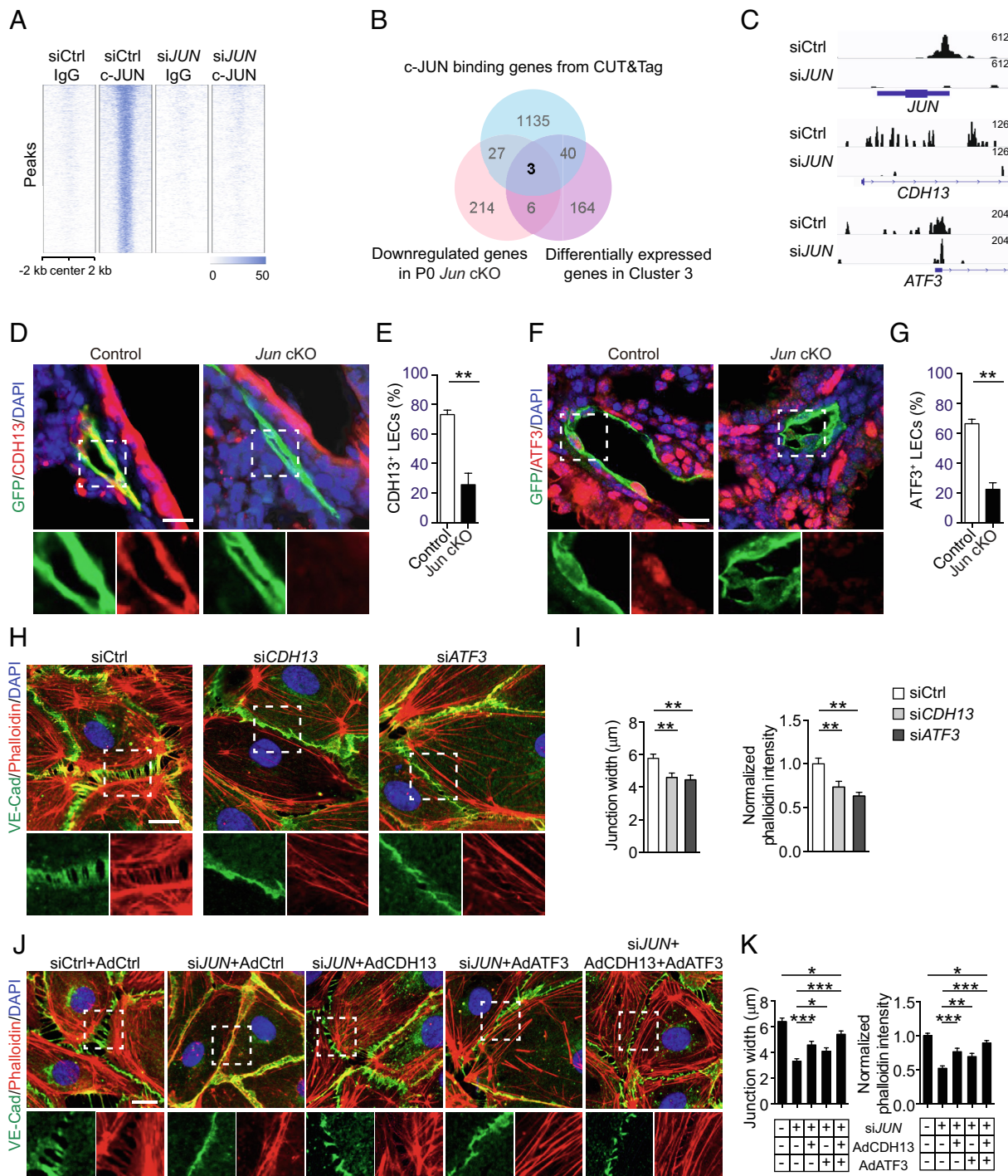

Fig. 4. c-JUN Promotes CDH13 and ATF3 Expression. (*A*) CUT&Tag analysis in siCtrl or si*JUN* LECs. Heatmaps showing immunoglobulin G (IgG) and c-JUN binding signals at 4-kb peak regions. (*B*) Venn diagram showing the overlap genes among three datasets: homologous mouse genes of c-JUN binding genes from CUT&Tag, downregulated genes in P0 *Jun* cKO LECs from bulk RNA-seq, and genes differentially expressed in Cluster 3 LECs from scRNA-seq. The Cluster 3 LECs highly expressed c-JUN. (*C*) IGV track view showing c-JUN binding signals at the loci of three genes from (*B*). (*D* and *E*) Lungs of P0 control and *Jun* cKO mice were stained with antibodies against GFP and CDH13 (*D*). The percentages of CDH13+ LECs were quantified (*E*) (mean ± SEM, n = 3). (*F* and *G*) Lungs of P0 control and *Jun* cKO mice were stained with antibodies against GFP and ATF3 (*F*). The percentages of ATF3+ LECs were quantified (*G*) (mean ± SEM, n = 3). (*H* and *I*) siCtrl, si*CDH13*, or si*ATF3* LECs were stained with phalloidin and an antibody against VE-Cad (*H*). The average junction width was quantified (*I*) (mean ± SEM, n ≥ 50 junctions). Relative average phalloidin intensity was quantified (*I*) (mean ± SEM, n ≥ 20 cells). (*J* and *K*) CDH13- or/and ATF3-overexpressed si*JUN* LECs were stained with phalloidin and an antibody against VE-Cad (*J*). The average junction width was quantified (*K*) (mean ± SEM, n ≥ 50 junctions). Relative average phalloidin intensity was quantified (*K*) (mean ± SEM, n ≥ 28 cells). (*P < 0.05, **P < 0.01, ***P < 0.001, Student's *t* test: *E*, *G*, and *I*. One-way ANOVA test: *K*. Scale bars: *D*, *F*, *H*, and *J*, 15 μm.)

P0 *Jun* cKO LECs and differentially expressed in Cluster 3 LECs (Fig. 4*B*). In addition to *Jun* itself, two potential transcriptional targets of c-JUN, Cadherin 13 (*Cdh13*) and activating transcription factor 3 (*Atf3*), were found to fit these criteria (Figs. 1*G* and 4*C* and *SI Appendix*, Fig. S5*C*). It has been shown that CDH13 acts as a negative regulator of intercellular adhesion in blood endothelial cells by regulating cytoskeleton organization (34, 35). ATF3, another member of the AP-1 family, regulates various cellular stress responses, including remodeling of the actin cytoskeleton (36).

We first assessed the expression of *Cdh13* and *Atf3* in LECs of control and *Jun* cKO lungs. The proportions of CDH13$^+$ LECs and ATF3$^+$ LECs decreased significantly in *Jun* cKO LECs at P0 (Fig. 4 *D–G*). In si*JUN* LECs, the expressions of CDH13 and ATF3 were almost abolished (*SI Appendix*, Fig. S5 *D–G*). Additionally, we analyzed the developmental expression pattern of CDH13 and ATF3. Lungs of *Prox1*-GFP mice were stained with antibodies against CDH13 or ATF3 at E16.5, E18.5, P0, P1, P2, and P62. The proportion of CDH13$^+$ LECs and ATF3$^+$ LECs significantly increased in P0 lungs and then quickly reduced to fewer than 34% from P1 (*SI Appendix*, Fig. S5 *H–K*). Together these results support that CDH13 and ATF3 are transiently upregulated by c-JUN in P0 LECs.

To investigate the functions of CDH13 and ATF3 in regulating the remodeling of the actin cytoskeleton, we designed siRNAs to knock down the expression of *CDH13* or *ATF3* in LECs (*SI Appendix*, Fig. S5 *D–G*). In si*CDH13* and si*ATF3* LECs, the lateral sides of most adjacent LECs were still held to each other (Fig. 4 *H* and *I*). Fewer jagged VE-Cad lines and actin fibers were observed between the lateral sides of si*CDH13* and si*ATF3* LECs (Fig. 4 *H* and *I*). We next overexpressed ATF3 and/or CDH13 in si*JUN* LECs to investigate if the cytoskeletal abnormalities observed in si*JUN* LECs can be rescued (*SI Appendix*, Fig. S5*L*). Overexpressing ATF3 and/or CDH13 partially rescued the cytoskeletal abnormalities, with increased width of cell junctions and actin fibers in *JUN* knockdown LECs (Fig. 4 *J* and *K*). Our results thus support that the c-JUN targets CDH13 and ATF3 to regulate the function of LECs during the transition from prenatal to postnatal life.

Discussion

The failed lung inflation and pulmonary edema phenotypes that we observed in *Jun* cKO mice were similar to the phenotypes previously reported for lymphatic vessel development deficiency mice, highlighting the critical function of c-JUN in regulating lymphatic vessel function at birth (5). In addition to the transient expression of c-JUN in P0 lungs, we also observed that the opening of LEC flaps is transiently enlarged in P0 lungs (Fig. 2 *J* and *K* and *SI Appendix*, Fig. S3 *J* and *K*) and noted that flap opening was severely impaired in *Jun* cKO mice. These findings together demonstrate that c-JUN-regulated flap opening is essential in enabling lymphatic vessels to take up interstitial fluid in P0 lungs.

Intriguingly, our scRNA-seq analysis revealed that P0 LECs display distinct features with active responses to mechanical stimulus. Interstitial mechanical pressure is proposed as the main force to drive the opening of lymphatic vessels (29, 37). A previous study showed that interstitial mechanical pressure in the lung dramatically increases within 2 h after birth and decreases to below atmospheric pressure by 5 h after birth (31). Given our

observation that increased mechanical pressure induces the expression of c-JUN in LECs, we conclude that the transient LEC flap opening in P0 lungs is driven by mechanical pressure-mediated c-JUN expression.

We have shown that the c-JUN-mediated transcriptional regulation is transiently activated in P0 LECs. In response to a variety of signaling, transcriptional factors can orchestrate a large network of molecules for directing spatial and temporal patterns of gene expression (38). Considering the essential role of lymphatic vessels at birth, it is not surprising that the function of LECs is regulated at the transcription level for ensuring an integrated lymphatic fluid clearance process. Two identified c-JUN targets in LECs, *Cdh13* and *Atf3*, are also transiently upregulated in P0 LECs and regulate remodeling of the actin cytoskeleton of LECs. However, overexpressing both CDH13 and ATF3 only partially rescued the abnormal remodeling of the actin cytoskeleton in si*JUN* LECs. It is thus tempting to speculate that—in addition to *Cdh13* and *Atf3*—other targets of c-JUN likely participate in regulating lymphatic functions at birth.

In this study, we only investigated the function of c-JUN in LECs. In addition to *Jun*, the expressions of several other members of AP-1 family, including *Junb*, *Jund*, *Fos*, *Fosb*, *Atf3*, and *Maff*, also significantly increased in P0 LECs. Among these seven AP-1 members, only *Jun* null and *Junb* null mice exhibit embryonic developmental defects and died before birth (39–41). Mice lacking *Jund*, *Fos*, *Fosb*, *Atf3*, or *Maff* gene can survive into adulthood, indicating that each of these AP-1 genes is dispensable for the lymphatic vessel functions at birth. We also compared the expression of AP-1 family genes between P0 control and *Jun* cKO mice. We found that the expression of other AP-1 family genes was not significantly different between control and *Jun* cKO LECs. This is consistent with previous studies showing that each AP-1 member has specific functions and shows no compensatory upregulation when other AP1 family gene was deleted (39). Whether JUNB and its targets participate in regulating lymphatic function at birth remains to be elucidated in the future.

Here we demonstrate that c-JUN-mediated transcriptional responses in LECs are essential for lung respiratory function during the transition from prenatal to postnatal life. These findings greatly expand our understanding of the molecular mechanisms of lymphatic clearance function. Stimulating the functions of lymphatic vessels has been proposed as a treatment to resolve lymphedema (42, 43). Our discoveries provide insights for future identifying targets for promoting lymphatic function during development and in diseases.

Author affiliations: ^{a}National Institute of Biological Sciences, Beijing 102206, China; ^{b}Graduate School of Peking Union Medical College, Beijing 100730, China; and ^{c}Tsinghua Institute of Multidisciplinary Biomedical Research, Tsinghua University, Beijing 100084, China

1. A. Hislop, E. Hey, L. Reid, The lungs in congenital bilateral renal agenesis and dysplasia. *Arch. Dis. Child.* **54**, 32–38 (1979).
2. J. Li *et al.*, The strength of mechanical forces determines the differentiation of alveolar epithelial cells. *Dev. Cell* **44**, 297–312.e5 (2018).
3. D. I. Tudehope, M. H. Smyth, Is "transient tachypnoea of the newborn" always a benign disease? Report of 6 babies requiring mechanical ventilation. *J. Paediatr. Child Health* **15**, 160–165 (1979).
4. L. Guglani, S. Lakshminrusimha, R. M. Ryan, Transient tachypnea of the newborn. *Pediatr. Rev.* **29**, e59–e65 (2008).

5. Z. Jakus *et al.*, Lymphatic function is required prenatally for lung inflation at birth. *J. Exp. Med.* **211**, 815–826 (2014).
6. K. Alitalo, T. Tammela, T. V. Petrova, Lymphangiogenesis in development and human disease. *Nature* **438**, 946–953 (2005).
7. T. Tammela, K. Alitalo, Lymphangiogenesis: Molecular mechanisms and future promise. *Cell* **140**, 460–476 (2010).
8. G. Oliver, J. Kipnis, G. J. Randolph, N. L. Harvey, The lymphatic vasculature in the 21st century: Novel functional roles in homeostasis and disease. *Cell* **182**, 270–296 (2020).
9. S. P. Williams *et al.*, Genome-wide functional analysis reveals central signaling regulators of lymphatic endothelial cell migration and remodeling. *Sci. Signal.* **10**, eaal2987 (2017).
10. J. E. Moore, C. D. Bertram, Lymphatic system flows. *Annu. Rev. Fluid Mech.* **50**, 459–482 (2018).
11. A. G. Warren, H. Brorson, L. J. Borud, S. A. Slavin, Lymphedema. *Ann. Plast. Surg.* **59**, 464–472 (2007).
12. X. Jiang, M. R. Nicolls, W. Tian, S. G. Rockson, Lymphatic dysfunction, leukotrienes, and lymphedema. *Annu. Rev. Physiol.* **80**, 49–70 (2018).
13. T. Mäkinen, L. M. Boon, M. Vikkula, K. Alitalo, Lymphatic malformations: Genetics, mechanisms and therapeutic strategies. *Circ. Res.* **129**, 136–154 (2021).
14. P. Baluk *et al.*, Functionally specialized junctions between endothelial cells of lymphatic vessels. *J. Exp. Med.* **204**, 2349–2362 (2007).
15. L. C. Yao, P. Baluk, R. S. Srinivasan, G. Oliver, D. M. McDonald, Plasticity of button-like junctions in the endothelium of airway lymphatics in development and inflammation. *Am. J. Pathol.* **180**, 2561–2575 (2012).
16. R. M. Kulkarni, A. Herman, M. Ikegami, J. M. Greenberg, A. L. Akeson, Lymphatic ontogeny and effect of hypoplasia in developing lung. *Mech. Dev.* **128**, 29–40 (2011).
17. I. Choi *et al.*, Visualization of lymphatic vessels by Prox1 -promoter directed GFP reporter in a bacterial artificial chromosome-based transgenic mouse. *Blood* **117**, 362–365 (2011).
18. C. Norrmén *et al.*, FOXC2 controls formation and maturation of lymphatic collecting vessels through cooperation with NFATc1. *J. Cell Biol.* **185**, 439–457 (2009).
19. D. Vittet, Lymphatic collecting vessel maturation and valve morphogenesis. *Microvasc. Res.* **96**, 31–37 (2014).
20. K. Nonomura *et al.*, Mechanically activated ion channel PIEZO1 is required for lymphatic valve formation. *Proc. Natl. Acad. Sci. U.S.A.* **115**, 12817–12822 (2018).
21. P. Angel, M. Karin, The role of Jun, Fos and the AP-1 complex in cell-proliferation and transformation. *Biochim. Biophys. Acta* **1072**, 129–157 (1991).
22. F. Hilberg, A. Aguzzi, N. Howells, E. F. Wagner, c-Jun is essential for normal mouse development and hepatogenesis. *Nature* **365**, 179–181 (1993).
23. R. Eferl *et al.*, Functions of c-Jun in liver and heart development. *J. Cell Biol.* **145**, 1049–1061 (1999).
24. G. Li *et al.*, c-Jun is essential for organization of the epidermal leading edge. *Dev. Cell* **4**, 865–877 (2003).
25. S. G. Hwang, S. S. Yu, S. W. Lee, J. S. Chun, Wnt-3a regulates chondrocyte differentiation via c-Jun/AP-1 pathway. *FEBS Lett.* **579**, 4837–4842 (2005).
26. G. Veluscek, Y. Li, S.-H. Yang, A. D. Sharrocks, Jun-mediated changes in cell adhesion contribute to mouse embryonic stem cell exit from ground state pluripotency. *Stem Cells* **34**, 1213–1224 (2016).
27. A. Wang *et al.*, Single-cell multiomic profiling of human lungs reveals cell-type-specific and age-dynamic control of SARS-CoV2 host genes. *Elife* **9**, e62522 (2020).
28. S. T. Proulx *et al.*, Use of a PEG-conjugated bright near-infrared dye for functional imaging of rerouting of tumor lymphatic drainage after sentinel lymph node metastasis. *Biomaterials* **34**, 5128–5137 (2013).
29. K. Aukland, R. K. Reed, Interstitial-lymphatic mechanisms in the control of extracellular fluid volume. *Physiol. Rev.* **73**, 1–78 (1993).
30. H. Wiig, M. A. Swartz, Interstitial fluid and lymph formation and transport: Physiological regulation and roles in inflammation and cancer. *Physiol. Rev.* **92**, 1005–1060 (2012).
31. G. Miserocchi, B. H. Poskurica, M. Del Fabbro, Pulmonary interstitial pressure in anesthetized paralyzed newborn rabbits. *J. Appl. Physiol.* **77**, 2260–2268 (1994).
32. L. Alderfer, E. Russo, A. Archilla, B. Coe, D. Hanjaya-Putra, Matrix stiffness primes lymphatic tube formation directed by vascular endothelial growth factor-C. *FASEB J.* **35**, 1–15 (2021).
33. T. Yeung *et al.*, Effects of substrate stiffness on cell morphology, cytoskeletal structure, and adhesion. *Cell Motil. Cytoskeleton* **60**, 24–34 (2005).
34. M. Philippova, D. Ivanov, V. Tkachuk, P. Erne, T. J. Resink, Polarisation of T-cadherin to the leading edge of migrating vascular cells in vitro: A function in vascular cell motility? *Histochem. Cell Biol.* **120**, 353–360 (2003).
35. M. Philippova *et al.*, RhoA and Rac mediate endothelial cell polarization and detachment induced by T-cadherin. *FASEB J.* **19**, 588–590 (2005).
36. X. Yuan *et al.*, ATF3 suppresses metastasis of bladder cancer by regulating gelsolin-mediated remodeling of the actin cytoskeleton. *Cancer Res.* **73**, 3625–3637 (2013).
37. H. Wiig, M. A. Swartz, Interstitial fluid and lymph formation and transport: Physiological regulation and roles in inflammation and cancer. *Physiol. Rev.* **92**, 1005–1060 (2012).
38. B. Lemon, R. Tjian, Orchestrated response: A symphony of transcription factors for gene control. *Genes Dev.* **14**, 2551–2569 (2000).
39. W. Jochum, E. Passegué, E. F. Wagner, AP-1 in mouse development and tumorigenesis. *Oncogene* **20**, 2401–2412 (2001).
40. M. G. Hartman *et al.*, Role for activating transcription factor 3 in stress-induced β-cell apoptosis. *Mol. Cell. Biol.* **24**, 5721–5732 (2004).
41. H. Yamazaki, F. Katsuoka, H. Motohashi, J. D. Engel, M. Yamamoto, Embryonic lethality and fetal liver apoptosis in mice lacking all three small Maf proteins. *Mol. Cell. Biol.* **32**, 808–816 (2012).
42. D. S. C. Ko, Effective treatment of lymphedema of the extremities. *Arch. Surg.* **133**, 452 (1998).
43. C. Norrmén, T. Tammela, T. V. Petrova, K. Alitalo, Biological basis of therapeutic lymphangiogenesis. *Circulation* **123**, 1335–1351 (2011).